



HAL
open science

Structural composite laminate materials with low dielectric loss: Theoretical model towards dielectric characterization

Maëlle Sergolle, Xavier Castel, Mohamed Himdi, Philippe Besnier, Patrick Parneix

► **To cite this version:**

Maëlle Sergolle, Xavier Castel, Mohamed Himdi, Philippe Besnier, Patrick Parneix. Structural composite laminate materials with low dielectric loss: Theoretical model towards dielectric characterization. Composites Part C: Open Access, 2020, 3, pp.100050. <10.1016/j.jcomc.2020.100050>. <hal-02971767>

HAL Id: hal-02971767

<https://hal.science/hal-02971767v1>

Submitted on 19 Oct 2020

HAL is a multi-disciplinary open access archive for the deposit and dissemination of scientific research documents, whether they are published or not. The documents may come from teaching and research institutions in France or abroad, or from public or private research centers.

L'archive ouverte pluridisciplinaire **HAL**, est destinée au dépôt et à la diffusion de documents scientifiques de niveau recherche, publiés ou non, émanant des établissements d'enseignement et de recherche français ou étrangers, des laboratoires publics ou privés.



HAL Authorization



Structural composite laminate materials with low dielectric loss: Theoretical model towards dielectric characterization



Maëlle Sergolle^{a,*}, Xavier Castel^a, Mohamed Himdi^a, Philippe Besnier^a, Patrick Parneix^b

^a Univ Rennes, INSA Rennes, CNRS, IETR-UMR 6164, F-35000 Rennes, France

^b Naval Group, Technocampus Océan, 44340 Bouguenais, France

ARTICLE INFO

Keywords:

Composite materials
Dielectric characterization
Maxwell-Garnett model
Microwaves

ABSTRACT

Organic matrix composite materials exhibit high mechanical properties associated with lightweight. They also provide the ability to embed radiofrequency features, such as microwave antennas, for smart load-bearing structures of various means of transport. Antennas implementation into composite panels requires electrically conductive fabrics for the radiating elements, feeding lines and ground planes embedded into the structural dielectric composite materials with low loss at microwaves. Accordingly, the present study investigates the assessment of the dielectric characteristics, namely the relative permittivity ϵ_r and the loss tangent $\tan\delta$ of composite laminate materials made of E-glass, S2-glass and quartz fabrics infused with epoxy, polyester and urethane acrylate thermosetting resins. The related dielectric characteristics, measured in two operating bands, namely 100 MHz to 1 GHz and 18–26 GHz, are compared with the theoretical values computed from the 2D Maxwell-Garnett model that we have adapted to laminate composite materials. Mechanical characteristics of such composite laminate materials are also investigated. Eventually, the quartz/urethane acrylate laminate is highlighted as a low loss composite material, highly suitable for the fabrication of antennas operating at microwaves.

1. Introduction

Organic matrix composite materials are increasingly used in transport area. These materials are mainly made of reinforcement fibers infused with thermosetting resins. They enable the fabrication of lightweight and mechanically resistant structural panels. Moreover, they promote embedded electronic applications. The vast area of Multifunctional Structures (MFS) [1] shows the interest of combining the functional capabilities of one or more subsystems with that of the load-bearing structure, thereby reducing the mass and volume of the total system [2]. Among clean energy production structures [3], integrated electronics [4] and smart structures [5], composite panels for radiofrequency communications have a prominent place in such multifunctional structure field.

Antennas implementation into load-bearing composite panels is a major aspect of the smart composite materials development. Various studies have already developed this innovative concept. Kim *et al.* [6] fabricated a multiband aero-vehicle smart skin antenna (MASSA) made of a single honeycomb including the radiating element stacked between two structural composite face sheets. This antenna can be integrated in the airplane load-bearing structure and operates close to 300 MHz. Manac'h *et al.* [7] demonstrated similar microwave performance between a pure composite laminate antenna and a copper one

operating both in the 600 MHz to 2.1 GHz frequency band. You *et al.* built conformal load-bearing antenna structures (CLAS) by integrating slots [8] and radiating patches [5] between two layers of honeycomb. The first structure resonates at 5.3 GHz and the second one operates at 12.2 GHz. In these works, a twofold study was carried out, (i) on the conductive fabrics to minimize the ohmic loss and the skin depth loss [7], and (ii) on the dielectric materials to minimize the dielectric loss [5,6,8]. The main objective of such studies aims to develop embedded communicating systems with optimal radiofrequency efficiency at microwaves. The present study focuses with the framework of the case (ii), namely the dielectric loss reduction of the dielectric composite materials. To date, the fibers reinforced dielectric laminates used for antenna applications are based on the twosome formed by E-glass/polyester [7], E-glass/vinylester [9,10], E-glass/epoxy [5,11,12], or S-glass/epoxy [13], as displayed in Table 1. The relative permittivity of such composite laminates remains close to $\epsilon_r \approx 4$ and the loss tangent $\tan\delta$ higher than 0.01, relatively high values for applications at microwaves.

The present paper investigates theoretically and experimentally various dielectric composite laminates made of glass fabrics and organic thermosetting resins, that may be used as load-bearing composite panels with low dielectric loss for antenna substrate and/or radome applications. After the description of the dielectric and mechanical characterization techniques, the glass fabrics used (namely E-glass, S2-glass and

* Corresponding author.

E-mail address: maelle.sergolle@univ-rennes1.fr (M. Sergolle).

Table 1
Dielectric characteristics of the fibers reinforced dielectric laminates used for antenna applications.

Composite laminate materials	L-band	S-band	X-band	V-band
E-glass/Polyester [7]	$\epsilon_r = 4.5$; $\tan\delta = 0.01$ @ 1 GHz	/	/	/
E-glass/Vinylester [9,10]	$\epsilon_r = 4.5$; $\tan\delta \approx 0.015$ @ 1.5 GHz	/	/	/
E-glass/Epoxy [5,11,12]	/	$\epsilon_r = 4.0$; $\tan\delta = 0.03$ @ 2.5 GHz	$\epsilon_r = 4.0$; $\tan\delta = 0.03$ @ 12 GHz	$\epsilon_r = 4.6$; $\tan\delta = 0.035$ @ 50-75 GHz
S-glass/Epoxy [13]	/	/	$\epsilon_r = 4.3$; $\tan\delta = 0.02$ @ 10 GHz	/

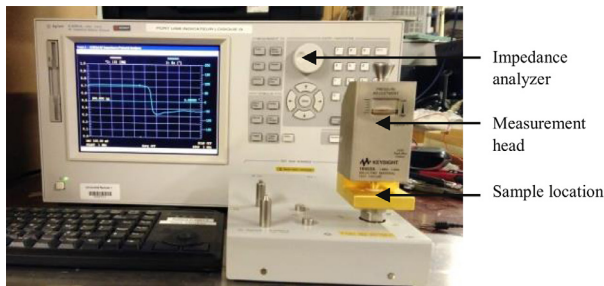


Fig. 1. Complex dielectric characterization by impedance measurement.

fused quartz fibers) and the thermosetting resins used (namely epoxy, polyester and urethane acrylate) are described, as well as the implementation process. Then, a two-dimensional Maxwell-Garnett model is presented and developed for our specific composite laminates to compute their dielectric characteristics (relative permittivity ϵ_r and loss tangent $\tan\delta$). The dielectric measurements are carried out over two frequency bands (100 MHz to 1 GHz and 18–26 GHz). Theoretical and experimental results are then compared and discussed. The mechanical characterization of the composite laminates, through tensile tests, completes the study. Finally, conclusions are drawn.

2. Characterization techniques

2.1. Dielectric characterization

Relative permittivity $\epsilon_r = \epsilon'_r$ and loss tangent $\tan\delta = \epsilon''_r / \epsilon'_r$ are displayed from the complex dielectric permittivity expression $\epsilon^* = \epsilon'_r - j\epsilon''_r$. ϵ^* is retrieved from two separate techniques, namely the impedance measurement and the free-space measurement. For each type of composite laminates, three different samples machined from the same laminate are assessed.

2.1.1. Impedance measurement

The impedance measurement (Fig. 1) retrieves ϵ_r and $\tan\delta$ values from 100 MHz to 1 GHz. An impedance analyzer is connected to a measurement head. The measurement head acts as a capacitor of 7 mm-diameter. Prior to measurements, a standard calibration was carried out through an open (non-contact capacitor plates), short (face-to-face contact capacitor plates), and load (25 mm \times 25 mm \times 0.8 mm Teflon[®] sample with $\epsilon_r = 2.08$ over the entire frequency band) sequential steps. The sample surfaces have to be smooth to prevent any air gap between the sample face and the related capacitor plate (which would cause artifacts). The measurement uncertainties are provided by the measurement accuracy of the apparatus, as given by the supplier [14].

2.1.2. Free-space measurement

The free-space measurement (Fig. 2) retrieves ϵ_r and $\tan\delta$ values from 18 to 26 GHz. This technique is based on the signal processing of reflection/transmission electromagnetic plane waves illuminating the sample under test. A transmitting horn antenna, connected to a network analyzer, radiates an electromagnetic field which is focused as a (locally) plane wave on the sample by the use of two successive reflective mirrors.

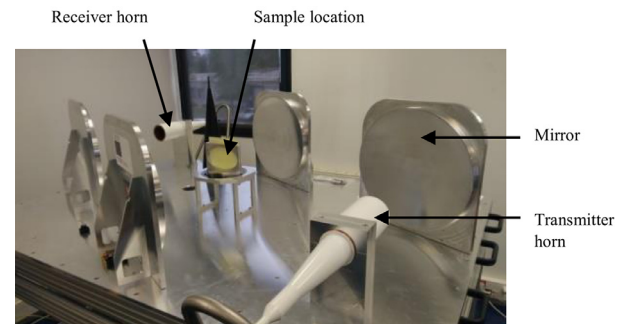


Fig. 2. Complex dielectric characterization by free-space measurement.

The incident plane waves undergo reflection and transmission through the sample under test according to its dielectric properties. The second horn receives the outgoing electromagnetic waves after their reflection onto two new successive mirrors. Prior to measurements, calibration was also carried out through a standard thru (no sample), reflect (metal plate), load (150 mm \times 150 mm \times 6.7 mm Teflon[®] sample with $\epsilon_r = 2.09$ over the entire frequency band) sequential steps. For this technique, the measurement uncertainties are mostly related to the sample thickness spreading. A same sample of composite laminate material fabricated by the vacuum infusion process may exhibit a thickness variation of about ± 0.2 mm on 150 mm \times 150 mm sample area. Due to this uncertainty, results of free space measurement exhibit a relative permittivity variation of 8% and a loss tangent variation of 11% at 18 GHz.

2.2. Mechanical characterization by tensile tests

To evaluate the mechanical characteristics of the composite laminate materials, tensile tests were performed up to the sample rupture, according to the mechanical standard [15]. A Lloyd Instruments testing machine (LR50K Plus) was used with a constant displacement rate of 2 mm/min applied on 25 mm-width and 250 mm-length samples. Resulting force was measured with a 50 kN-force sensor and sample elongation was measured through the variation of a random speckle pattern applied on each sample surface and monitored by a camera. The related strain, defined as $(L-L_0)/L_0$ where L is the length of the sample during the test and L_0 is the initial length of the sample, was computed with the Digital Image Correlation (DIC) method [16]. The resulting tensile elastic modulus (Young modulus) was retrieved between 100 and 200 MPa (curve slope). The behavior of each type of composite laminates was averaged from 5 samples measurements.

3. Fabrics, thermosetting resins and their implementation

3.1. Reinforcement fibers and the related fabrics

Among the families of inorganic reinforcement fibers and the related fabrics, fibers of E-glass, S2-glass and fused quartz (commonly known as “quartz”) were selected here according to their attractive dielectric characteristics and their common use in the field of composite materials. E-glass fibers are the most popular reinforcements used in the transportation area. They are mainly made of silica (55%wt. SiO₂) and

Table 2

Dielectric characteristics (ϵ_f , $\tan\delta_f$) at 100 MHz and 1 GHz of the selected reinforcement fibers, estimated from [18].

Fibers	ϵ_f		$\tan\delta_f$	
	100 MHz	1 GHz	100 MHz	1 GHz
Quartz	3.7	3.7	1.0×10^{-4}	1.1×10^{-4}
S2-glass	5.3	5.3	2.0×10^{-3}	2.5×10^{-3}
E-glass	6.4	6.4	3.0×10^{-3}	3.1×10^{-3}

calcium oxide (19%wt. CaO). The remaining 26%wt. are composed of others oxides, mainly Al_2O_3 , B_2O_3 and MgO. S2-glass contains a high content of silica (65%wt.), alumina (25%wt. Al_2O_3) and magnesium oxide (10%wt. MgO), and is known for its lower relative permittivity (Table 2) and its good mechanical strength [17]. Quartz fiber, made of 99.99%wt. pure silica, exhibits high temperature resistance as well as low dielectric characteristics values (Table 2, [18]). The relative permittivity ϵ_f and loss tangent $\tan\delta_f$ of the three types of fibers are displayed in Table 2.

In this study, a quadriaxial fabric of E-glass fibers (2.8 yarns/cm in the warp direction with an area density equal to 618 g/m², reference QX618 from Sicomin, France), a plain weave of S2-glass fibers (2.1 yarns/cm in the warp direction with an area density of 516 g/m², reference 6000 from CTMI, France) and a 4H-satin of quartz fibers (11 yarns/cm in the warp direction with an area density of 180 g/m², reference 5903 from CTMI, France) were used. The quadriaxial weave is a stack of four layers of unidirectional yarns: a first layer oriented at +45° to the warp direction, a second layer oriented at 90°, a third layer oriented at -45° and the top layer parallel to the warp direction (0°). The plain weave corresponds to a periodic interlacing of yarns, alternatively one over, one under. Finally, 4H-satin (four-harness satin) is a three by one interlacing pattern. According to the supplier data, the Young modulus of the E-glass and of the quartz fibers is equal to 72 GPa, and that of the S2-glass fibers is equal to 87 GPa. Literature reports an elongation at break of 4.5–5% for E-glass fibers [18], 5.4–5.8% for S2-glass fibers [18] and 8.7% for quartz fibers [19].

3.2. Thermosetting resins

In order to infuse the previous reinforcement fabrics to fabricate the composite laminate materials, three types of thermosetting resins were selected in the present study: the polyester, the epoxy and the urethane acrylate resins.

Polyester is the cheapest thermosetting resin and the most used in the field of composite materials, mainly in the fabrication of mainstream ships, cars and industrial parts. It is produced by a condensation reaction between a glycol and an unsaturated dibasic acid. The polyester resin polymerizes after adding a catalyst (an organic peroxide) and a cobalt accelerator [17]. In this study, the polyester resin used is a pre-accelerated Norester® 823 (Nord Composites, France) and was catalyzed with 2%wt. of catalyst (PMEC from Nord Composites, France). The resin was polymerized first at room temperature for 24 h, and then was cured at 40 °C for 16 h.

Epoxy is a two-component resin. This thermosetting resin is well known to achieve high mechanical and temperature resistance performance of composite laminates for high value-added products in various means of transport: ships, vehicles and aircraft [17]. In this study, epoxy resin (SR8100 from Sicomin, France), after adding hardener (SD8824 from Sicomin, France) with a 27:100 (v/v) ratio, was polymerized at room temperature for 24 h, followed by a curing step at 80 °C for 6 h.

Urethane acrylate resin is made of a monomer containing urethane groups with chain extenders. This resin is mainly used in the automotive sector, for the bumpers fabrication for example. In this study, as polyester resin, the urethane acrylate resin (Crestapol® 1261 from Scott Bader, UK), after adding first 2%wt. of cobalt accelerator (NL49P

Table 3

Measured dielectric characteristics (ϵ_m , $\tan\delta_m$) at 100 MHz and 1 GHz of the selected thermosetting resins (retrieved from impedance measurement)

Resin	$\epsilon_m (\pm 0.5)$		$\tan\delta_m (\pm 0.5 \times 10^{-3})$	
	100 MHz	1 GHz	100 MHz	1 GHz
Urethane acrylate	2.7	2.7	5×10^{-3}	5×10^{-3}
Polyester	2.7	2.6	1.4×10^{-2}	1.1×10^{-2}
Epoxy	3.3	3.1	3.0×10^{-2}	2.5×10^{-2}

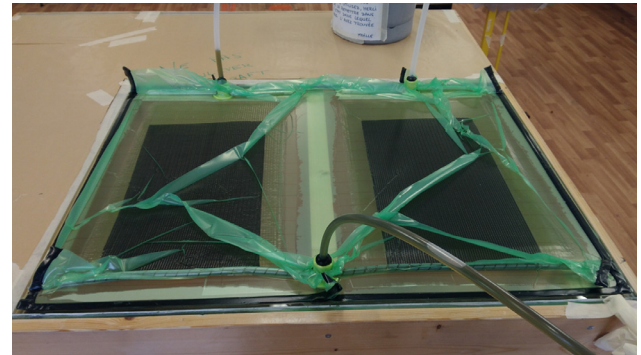


Fig. 3. Composite laminate material during its fabrication by vacuum infusion process.

from AkzoNobel Functional Chemicals, Netherlands) and then 2%wt. of specific catalyst (Trigonox 239 from AkzoNobel Functional Chemicals, Netherlands), was polymerized at room temperature for 24 h, followed by a curing step at 40 °C for 16 h.

The three thermosetting resins used in this study are infusion resins. Furthermore at room temperature, these resins are glassy polymers. According to the supplier data, the Young modulus of the polyester, epoxy and urethane acrylate resins is equal to 3 GPa, 2.4 GPa and 3.6 GPa, respectively.

The single resins were cast in silicon molds and cured for the relevant time. Impedance measurements on 2-mm thick samples were carried out (Table 3). Urethane acrylate resin exhibits the lowest values of dielectric characteristics in the 100 MHz to 1 GHz frequency range: $\epsilon_m = 2.7 \pm 0.5$ and $\tan\delta_m = 5.0 \times 10^{-3} \pm 0.5 \times 10^{-3}$.

3.3. Fabrication of the composite laminate materials

Samples fabrication was done by standard vacuum infusion process, widely used in industrial environment. It consists in infusing a fabric by a thermosetting resin under vacuum. In this way, dry fabrics were stacked onto a waxed glass slab. Placed under vacuum (-0.6 bar) with a plastic bag as shown in Fig. 3, fabrics were infused jointly with the liquid thermosetting resin. After 24 h of polymerization at room temperature followed by the suitable curing step, the composite laminate materials were cut to the required sizes to undergo the dielectric characterizations (25 mm × 25 mm × 2 mm for the impedance measurement; 150 mm × 150 mm × 2 mm for the free-space measurement) and the mechanical characterizations (250 mm × 25 mm × 2 mm).

The fiber volume fraction V_f of each sample was computed as follows:

$$V_f = \frac{n \times m_{of}}{\rho_f \times h} \quad (1)$$

where n is the number of plies of the dry reinforcement fabrics, m_{of} is the area density of the dry fabrics (kg/m²), ρ_f is the glass fiber volume density (kg/m³), and h is the measured thickness of the composite laminate sample (m).

Nine separate composite laminates (Table 4) were fabricated and investigated here, each made of specific reinforcement fabrics (E-glass, S2-

Table 4

Fiber volume fraction V_f of the fabricated composite laminate materials computed from Eq. (1) with $\rho_{\text{quartz}} = 2200 \text{ kg/m}^3$ and $\rho_{\text{E-glass}} = \rho_{\text{S2-glass}} = 2600 \text{ kg/m}^3$, n is the number of plies of the reinforcement fabric in each laminate, and h is the thickness of the composite laminate sample.

Composite laminate materials	n	$h \pm 0.2$ (mm)	V_f (%)
Quartz / Epoxy	12	2.3	42
Quartz / Polyester	12	2.4	42
Quartz / Urethane acrylate	12	2.4	41
S2-glass / Epoxy	5	2.1	46
S2-glass / Polyester	5	2.3	44
S2-glass / Urethane acrylate	5	2.3	43
E-glass / Epoxy	5	2.7	45
E-glass / Polyester	5	2.6	46
E-glass / Urethane acrylate	5	2.7	45

glass and quartz) infused with a specific thermosetting resin (polyester, epoxy and urethane acrylate).

4. Mixing rules in the 100 MHz to 1 GHz frequency range

Since the last century, researchers develop theoretical models, called effective medium approximations (EMA), to predict and compute theoretically the macroscopic relative permittivity ϵ_{eff} of composite materials made of a host medium (characterized by the relative permittivity ϵ_h and volume fraction V_h) and inclusions (characterized by the relative permittivity ϵ_i and volume fraction $V_i = 1 - V_h$).

4.1. Mixing rules without loss

From the Maxwell equations, Maxwell-Garnett built a theory of homogenization [20] based on a medium containing spherical inclusions, still widely used today [21–23]. Based on this theory, a three-dimensional mixing rule was developed to compute the effective permittivity (or the macroscopic relative permittivity) of the composite medium according to the relative permittivity of each component and its related volume fraction [24], as follows:

$$\epsilon_{\text{eff}} = \epsilon_h + 3V_i\epsilon_h \frac{\epsilon_i - \epsilon_h}{\epsilon_i + 2\epsilon_h - V_i(\epsilon_i - \epsilon_h)} \quad (2)$$

From a theoretical point of view, Bruggeman solved the problem of non-symmetry of the Maxwell-Garnett mixing rule (the results differed when ϵ_i and V_i were substituted by ϵ_h and V_h) [25]. Other studies led to an effective relative permittivity value covered by lower and upper bounds to take into account the phase distribution influence [26], or a relative permittivity value depending upon the fibers direction in relation with that of the applied electric field [27–29]. Nevertheless, all the previous models considered the composite media as lossless materials. Accordingly, the present study adapts a Maxwell-Garnett model considering composite media with dielectric loss.

4.2. 2D Maxwell-Garnett model of composite materials with dielectric loss

Sihvola developed a Maxwell-Garnett mixing rule which computed the complex dielectric permittivity $\epsilon^* = \epsilon_r - j \epsilon''_r$ of composite media without neglecting the loss, where the inclusion dimensions remained large compared with the molecular dimensions [30]. In the case of fiber reinforced composite laminates, this condition is obviously completely fulfilled. Moreover the fibers were considered as two-dimensional inclusions, as done by Bal and Kothari to predict the relative permittivity of non-infused polyethylene fabrics [28]. According to these considerations, the Maxwell-Garnett model was extended to two-dimensional composite media, namely the composite laminate materials, where the fibers of the reinforcement fabrics were considered as 2D cylinder dielectric inclusions embedded into a dielectric matrix. Because of the dielectric nature of the 2D cylinder fiber inclusions and of the matrix

[31], we assume that the complex permittivity ϵ^*_{comp} of the composite laminate materials can be expressed as follows [32]:

$$\epsilon^*_{\text{comp}} = \epsilon^*_m + 2V_f\epsilon^*_m \frac{\epsilon^*_f - \epsilon^*_m}{\epsilon^*_f + \epsilon^*_m - V_f(\epsilon^*_f - \epsilon^*_m)} \quad (3)$$

where ϵ^*_m is the complex permittivity of the resin host medium, ϵ^*_f is the complex permittivity of the fibers (2D inclusions), V_f is the fiber volume fraction, and $V_m = 1 - V_f$ is the matrix volume fraction in the composite laminate material. Eq. (3) complies the boundary conditions, namely $\epsilon^*_{\text{comp}} = \epsilon^*_m$ when $V_f = 0$ and $\epsilon^*_{\text{comp}} = \epsilon^*_f$ when $V_f = 1$. It is worth noting that porosity (with $\epsilon^*_{\text{air}} = 1$) into the composite laminate samples is neglected, which is close to reality when the vacuum infusion process is implemented to fabricate such samples. Moreover the model described above remains suitable if the wavelength of the electromagnetic field used to characterize the composite material is large enough in comparison with the dispersion and dimensions of the inclusions. These conditions then enable the modelling of the diffusion effects as coming from an equivalent homogeneous material. At 3 GHz, the working wavelength of the electromagnetic field equals 10 cm. The biggest fabric yarn used is 0.5 cm-wide (S2-glass – 2.1 yarns/cm) with a repeat weave unit of 1 cm-wide. Therefore to consider the composite laminate material as a homogeneous material for an electromagnetic point of view, the present model is no longer suitable beyond the 3 GHz limit-frequency. Accordingly, the mixing rule has been applied in the 100 MHz to 1 GHz frequency range.

4.3. Application of the 2D Maxwell-Garnett model to the composite laminate materials

The 2D Maxwell-Garnett model was used to compute the complex dielectric permittivity ϵ^*_{comp} (Eq. (3)) of the composite laminate materials from the complex dielectric permittivity values of the reinforcement fibers ϵ^*_f (Table 2) and of the single thermosetting resins ϵ^*_m (Table 3), and by taking into account the fiber volume fraction V_f in the composite laminate samples (Table 4). Results are displayed in Table 5 at both ends of the studied frequency band, namely 100 MHz and 1 GHz.

On the one hand, the relative permittivity values of the single thermosetting resins range from 2.6–2.7 (polyester and urethane acrylate resins) to 3.1–3.3 (epoxy resin) in the 100 MHz to 1 GHz frequency band, inducing an amplitude deviation $\Delta\epsilon_m = 0.6$ at 100 MHz and $\Delta\epsilon_m = 0.5$ at 1 GHz (Table 3). For the relative permittivity values of the reinforcement fibers, they range from 3.7 (quartz fibers) to 6.4 (E-glass fibers) in the working frequency band, inducing higher values and larger amplitude deviation ($\Delta\epsilon_f = 2.7$) (Table 2). Accordingly the computed relative permittivity values $\epsilon_{r \text{ comp}}$ of the composite laminate materials are controlled by the type of reinforcement fibers used and they can be grouped in three families whatever the working frequency (Table 5): the E-glass fiber reinforced laminates with $\epsilon_{r \text{ comp}}$ ranging from 3.9 to 4.5; the S2-glass fiber reinforced laminates with $\epsilon_{r \text{ comp}}$ ranging from 3.5 to 4.1; and the quartz fiber reinforced laminates with $\epsilon_{r \text{ comp}}$ ranging from 3.0 to 3.5. Within each family, the composite laminates with epoxy resin host medium always exhibit the relative higher $\epsilon_{r \text{ comp}}$ values while the ones with polyester and urethane acrylate host media are close together (in agreement with their related ϵ_m values).

On the other hand, loss tangent $\tan\delta_m$ values of the single thermosetting resins range from 5×10^{-3} (urethane acrylate) to $25\text{--}30 \times 10^{-3}$ (epoxy) with a ratio equal to 6 (Table 3) and those of the reinforcement fibers from 0.1×10^{-3} (quartz) to 3×10^{-3} (E-glass, Table 2) in the 100 MHz to 1 GHz frequency band. Despite the ratio variation of the reinforcement fiber $\tan\delta_f$ values, loss tangent of the composite laminates is controlled by the type of the thermosetting resin used due to their relative high values, and can also be grouped in three families (Table 5): laminates with epoxy host medium ($\tan\delta_{\text{comp}}$ higher than 10^{-2}); laminates with polyester host medium ($6 \times 10^{-3} < \tan\delta_{\text{comp}} < 10^{-2}$); and laminates with urethane acrylate host medium ($\tan\delta_{\text{comp}}$ lower than 5×10^{-3}). For each family, the theoretical loss tangent values increase

Table 5

Theoretical complex permittivity ϵ_{comp}^* and loss tangent $\tan\delta_{comp}$ of the composite laminate materials computed from the 2D Maxwell-Garnett model at 100 MHz and 1 GHz.

100 MHz		Quartz	S2-glass	E-glass
Epoxy	ϵ_{comp}^*	$3.48 - j 6.0 \times 10^{-2}$	$4.11 - j 7.2 \times 10^{-2}$	$4.43 - j 8.3 \times 10^{-2}$
	$\tan\delta_{comp}$	17.2×10^{-3}	17.4×10^{-3}	18.6×10^{-3}
Polyester	ϵ_{comp}^*	$3.09 - j 2.0 \times 10^{-2}$	$3.62 - j 3.2 \times 10^{-2}$	$3.96 - j 3.7 \times 10^{-2}$
	$\tan\delta_{comp}$	8.1×10^{-3}	8.9×10^{-3}	9.4×10^{-3}
Urethane acrylate	ϵ_{comp}^*	$3.10 - j 1.0 \times 10^{-2}$	$3.61 - j 1.4 \times 10^{-2}$	$3.94 - j 1.7 \times 10^{-2}$
	$\tan\delta_{comp}$	3.1×10^{-3}	3.9×10^{-3}	4.3×10^{-3}
1 GHz		Quartz	S2-glass	E-glass
Epoxy	ϵ_{comp}^*	$3.36 - j 2.5 \times 10^{-2}$	$3.97 - j 5.9 \times 10^{-2}$	$4.27 - j 6.7 \times 10^{-2}$
	$\tan\delta_{comp}$	14.3×10^{-3}	14.9×10^{-3}	15.8×10^{-3}
Polyester	ϵ_{comp}^*	$3.04 - j 2.0 \times 10^{-2}$	$3.55 - j 2.7 \times 10^{-2}$	$3.88 - j 3.1 \times 10^{-2}$
	$\tan\delta_{comp}$	6.6×10^{-3}	7.7×10^{-3}	7.9×10^{-3}
Urethane acrylate	ϵ_{comp}^*	$3.07 - j 0.9 \times 10^{-2}$	$3.57 - j 1.4 \times 10^{-2}$	$3.90 - j 1.7 \times 10^{-2}$
	$\tan\delta_{comp}$	3.1×10^{-3}	4.0×10^{-3}	4.3×10^{-3}

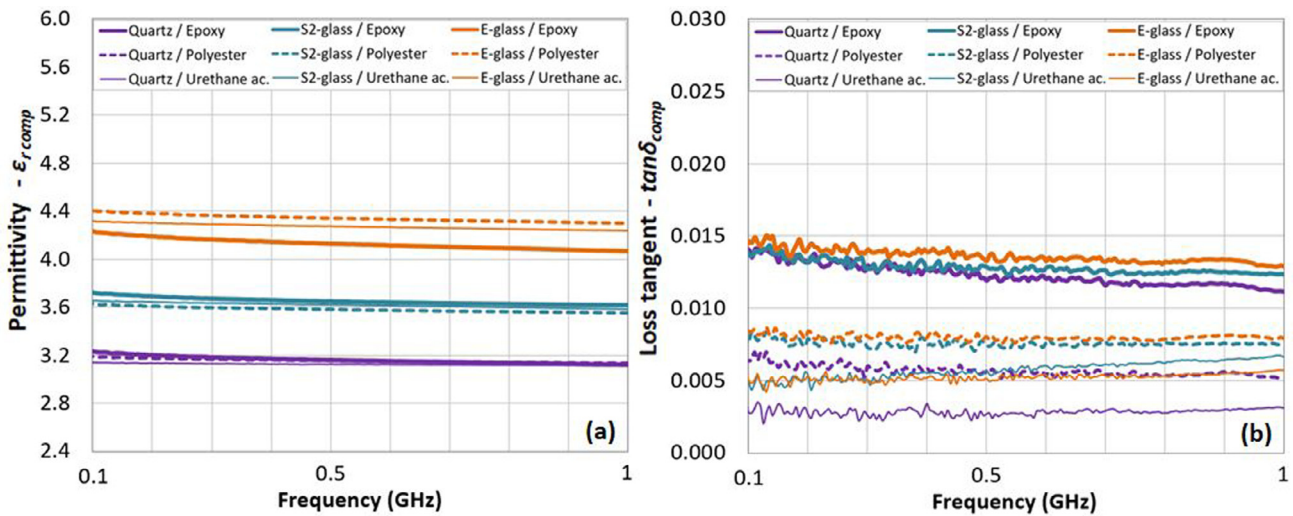


Fig. 4. 100 MHz to 1 GHz frequency variations of the relative permittivity $\epsilon_{r comp}$ (a) and loss tangent $\tan\delta_{comp}$ (b) of the composite laminate samples measured by impedance technique.

slightly according to the type of fibers (in agreement with their related loss tangent values), but without really affecting their related absolute value.

5. Characterizations of the composite laminate samples

5.1. Dielectric characterizations

5.1.1. Impedance measurement

Impedance measurement from 100 MHz to 1 GHz was performed on the nine studied composite laminate samples (E-glass, S2-glass, and quartz fibers, infused one by one with epoxy, polyester and urethane acrylate thermosetting resins). Fig. 4 presents ($\epsilon_{r comp}$; $\tan\delta_{comp}$) variations versus frequency of the composite laminate samples. ϵ_{comp}^* and $\tan\delta_{comp}$ at 100 MHz and 1 GHz are given in Table 7. As expected, the relative permittivity $\epsilon_{r comp}$ measurement identifies three composite laminate families, namely the E-glass reinforced laminates with the highest $\epsilon_{r comp}$ values ($\epsilon_{r comp} \approx 4.1$ – 4.4), the S2-glass reinforced laminates with the middle $\epsilon_{r comp}$ values ($\epsilon_{r comp} \approx 3.6$ – 3.7), and the quartz reinforced laminates with the lowest $\epsilon_{r comp}$ values ($\epsilon_{r comp} \approx 3.1$ – 3.2) in good agreement with the theoretical behavior resulting from the 2D Maxwell-Garnett model application. The relative permittivity values slightly decrease from 100 MHz to 1 GHz, as expected for standard dielectric materials [33].

Focusing on the dielectric loss, Fig. 4.b presents a relatively moderate variation of $\tan\delta_{comp}$ versus frequency for all the samples; it may be assumed as a constant for practical applications. The composite laminate samples infused with epoxy resin exhibits always the highest loss values ($\tan\delta_{comp}$ higher than 10^{-2} over the frequency band). E-glass and S2-glass/polyester laminate samples show higher loss than that of laminates infused with urethane acrylate resin. Loss tangent of quartz/polyester laminates remains close to that of the E-glass and S2-glass/urethane acrylate laminates. Accordingly, combination of middle loss reinforcement fibers with a low loss thermosetting resin is similar to the combination of low loss reinforcement fibers with middle loss thermosetting resin. Therefore, the combination of low loss reinforcement fibers with a low loss thermosetting resin, namely quartz/urethane acrylate laminate sample, must exhibit the lowest dielectric loss over the entire frequency band: $\tan\delta_{comp} = 2.8 \times 10^{-3}$ at 100 MHz and $\tan\delta_{comp} = 3.1 \times 10^{-3}$ at 1 GHz.

5.1.2. Free-space measurement

The dielectric characterizations were supplemented by free-space measurement from 18 to 26 GHz on the same composite laminate samples (Fig. 5).

As at lower frequencies (100 MHz to 1 GHz), the results from free-space measurement specify three composite laminate families, regardless of the resins used: the E-glass fiber reinforced laminates with $\epsilon_{r comp}$ ranging from 4.3 to 5.0; the S2-glass fiber reinforced laminates with

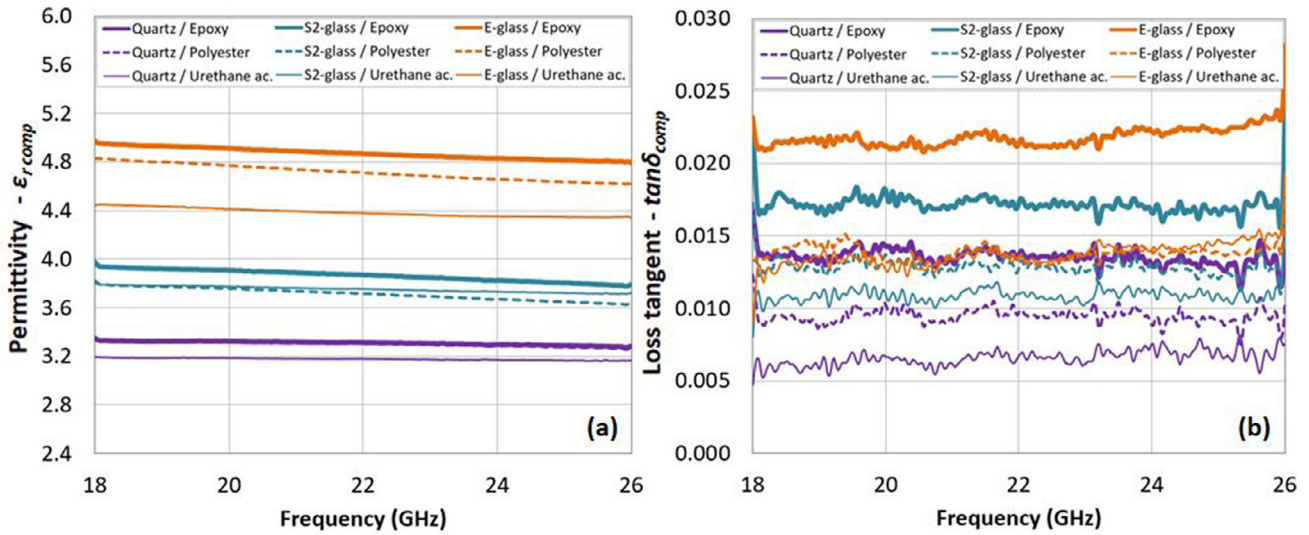


Fig. 5. 18-26 GHz frequency variations of the relative permittivity $\epsilon_{r,comp}$ (a) and loss tangent $\tan\delta_{comp}$ (b) of the composite laminate samples measured by free-space technique.

Table 6
Young modulus (GPa) of the composite laminate materials.

Young modulus	Quartz	S2-glass	E-glass
Epoxy	18.1 ± 0.7	21.1 ± 0.9	12.9 ± 1.2
Polyester	17.4 ± 0.5	20.6 ± 0.7	12.4 ± 0.4
Urethane acrylate	16.5 ± 0.5	19.5 ± 0.5	12.1 ± 1.1

$\epsilon_{r,comp}$ ranging from 3.6 to 4.0; and the quartz fiber reinforced laminates with $\epsilon_{r,comp}$ ranging from 3.1 to 3.4. Comparison of the absolute relative permittivity values from free-space measurement with those from impedance measurement exhibits an increasing $\epsilon_{r,comp}$ value from 1 GHz to 18 GHz. This increase is ascribed to the own uncertainties of the two separate techniques used to characterize the samples in two different frequency bands. As a reminder, the impedance measurement is based on a capacitive method while free-space measurement is based on an electromagnetic reflection/transmission waves method. Nevertheless, the expected decrease of $\epsilon_{r,comp}$ values is noticed from 18 GHz to 26 GHz.

Focusing now on the loss tangent variations versus frequency, $\tan\delta_{comp}$ values exhibiting by the nine samples are less split from each other than at lower frequencies. However, the same trends are observed: first, the direct impact of the resin type on the dielectric loss of the composite laminates, and second, the slight influence of the reinforcement fibers type on their dielectric loss. Accordingly, E-glass/epoxy laminates exhibit the highest dielectric loss with $\tan\delta_{comp}$ higher than 2×10^{-2} over the entire 18–26 GHz frequency band while quartz/urethane acrylate laminates exhibit once more the lowest dielectric loss with $\tan\delta_{comp}$ lower than 8×10^{-3} .

5.2. Mechanical characterization

The stress-strain curves (Fig. 6) highlight a pure elastic behavior of the nine composite laminates. Moreover the use of quartz fiber reinforcement shows an increase of the elongation at break (up to 3.6%), while the composite laminates reinforced with S2-glass and E-glass fibers exhibit a similar elongation at break (close to 2.7%). This result is explained by the intrinsic elongation at break of the pure glass fibers (as a reminder, 8.7% for quartz fibers, 5.4–5.8% for S2-glass fibers and 4.5–5% for E-glass fibers). Regarding the stiffness of the samples studied (Table 6), the composite laminates reinforced with S2-glass fibers exhibit a Young modulus close to 20 GPa, those reinforced with quartz fibers close to 17 GPa, and those reinforced with E-glass fibers close to

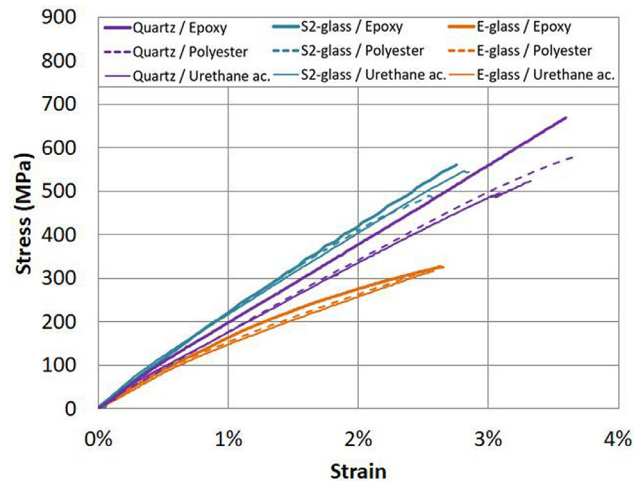


Fig. 6. Stress-strain curves of the composite laminate samples measured from tensile test.

12 GPa. It is worth noting that, even though epoxy resin provides a slight increase in stiffness of the composite laminates, the impact of the resin used is not relevant on their absolute Young modulus value. This result stems from the similar mechanical characteristics of the pure resins used (as a reminder, Young modulus equals 2.4 GPa for epoxy resin, 3 GPa for polyester resin and 3.6 GPa for urethane acrylate resin).

6. Comparison of the 2D Maxwell-Garnett model with the microwave measurements

($\epsilon_{r,comp}; \tan\delta_{comp}$) values retrieved from impedance measurement are compared with those computed from Eq. (3) of the tailored 2D Maxwell-Garnett model at 100 MHz and 1 GHz (Table 7). Theoretical $\epsilon_{r,comp}$ values always fit with the measured ones in the uncertainty range of measurement. The theoretical $\tan\delta_{comp}$ values often exhibit slightly higher levels than the measured ones. Nevertheless, theoretical and measured values remain very close to each other. Therefore, the proposed 2D Maxwell-Garnett model provides fair ($\epsilon_{r,comp}; \tan\delta_{comp}$) theoretical values of the low loss composite laminate materials, conditionally upon the electromagnetic wavelength used is large enough compared with the dispersion and dimension scales of the reinforcement fibers.

Table 7Comparison of the computed and measured ($\epsilon_{r, comp}$; $\tan\delta_{comp}$) dielectric characteristics of the composite laminate materials at 100 MHz and 1 GHz.

Composite laminate materials	Theoretical $\epsilon_{r, comp}$	Measured $\epsilon_{r, comp}$	Theoretical $\tan\delta_{comp}$	Measured $\tan\delta_{comp}$
100 MHz				
Quartz / Epoxy	3.48	3.2 ± 0.5	17.2 × 10 ⁻³	14.0 × 10 ⁻³ ± 0.5 × 10 ⁻³
Quartz / Polyester	3.09	3.2 ± 0.5	8.1 × 10 ⁻³	6.4 × 10 ⁻³ ± 0.5 × 10 ⁻³
Quartz / Urethane acrylate	3.10	3.1 ± 0.5	3.1 × 10⁻³	2.8 × 10⁻³ ± 0.5 × 10⁻³
S2-glass / Epoxy	4.11	3.7 ± 0.5	17.4 × 10 ⁻³	13.7 × 10 ⁻³ ± 0.5 × 10 ⁻³
S2-glass / Polyester	3.62	3.6 ± 0.5	8.9 × 10 ⁻³	7.6 × 10 ⁻³ ± 0.5 × 10 ⁻³
S2-glass / Urethane acrylate	3.61	3.7 ± 0.5	3.9 × 10 ⁻³	4.8 × 10 ⁻³ ± 0.5 × 10 ⁻³
E-glass / Epoxy	4.43	4.2 ± 0.6	18.6 × 10 ⁻³	14.6 × 10 ⁻³ ± 0.5 × 10 ⁻³
E-glass / Polyester	3.96	4.4 ± 0.6	9.4 × 10 ⁻³	8.4 × 10 ⁻³ ± 0.5 × 10 ⁻³
E-glass / Urethane acrylate	3.94	4.3 ± 0.6	4.3 × 10 ⁻³	5.0 × 10 ⁻³ ± 0.5 × 10 ⁻³
1 GHz				
Quartz / Epoxy	3.36	3.1 ± 0.5	14.3 × 10 ⁻³	11.1 × 10 ⁻³ ± 0.5 × 10 ⁻³
Quartz / Polyester	3.04	3.1 ± 0.5	6.6 × 10 ⁻³	5.2 × 10 ⁻³ ± 0.5 × 10 ⁻³
Quartz / Urethane acrylate	3.07	3.1 ± 0.5	3.1 × 10⁻³	3.1 × 10⁻³ ± 0.5 × 10⁻³
S2-glass / Epoxy	3.97	3.6 ± 0.5	14.9 × 10 ⁻³	12.3 × 10 ⁻³ ± 0.5 × 10 ⁻³
S2-glass / Polyester	3.55	3.6 ± 0.5	7.7 × 10 ⁻³	7.6 × 10 ⁻³ ± 0.5 × 10 ⁻³
S2-glass / Urethane acrylate	3.57	3.6 ± 0.5	4.0 × 10 ⁻³	6.6 × 10 ⁻³ ± 0.5 × 10 ⁻³
E-glass / Epoxy	4.27	4.1 ± 0.6	15.8 × 10 ⁻³	12.9 × 10 ⁻³ ± 0.5 × 10 ⁻³
E-glass / Polyester	3.88	4.3 ± 0.6	7.9 × 10 ⁻³	8.0 × 10 ⁻³ ± 0.5 × 10 ⁻³
E-glass / Urethane acrylate	3.90	4.2 ± 0.6	4.3 × 10 ⁻³	5.7 × 10 ⁻³ ± 0.5 × 10 ⁻³

Both theoretical and experimental investigations demonstrate that the reinforcement fibers type impacts the relative permittivity of the composite laminate materials, and the organic resin type impacts their dielectric loss. In that way, the quartz/urethane acrylate composite laminate exhibits the most attractive dielectric characteristics for microwave applications, namely low relative permittivity value ($\epsilon_{r, comp} = 3.1 \pm 0.5$) and very low loss value ($\tan\delta_{comp} \approx 2.9 \times 10^{-3} \pm 0.5 \times 10^{-3}$) in the 100 MHz to 1 GHz frequency band. This composite laminate can therefore be used as radome and/or dielectric substrate for antenna applications.

To date, cyanate ester resin was the most attractive resin in the aeronautical area due to its high dielectric and mechanical performance. This resin is an epoxy-like processing, but more difficult to implement due to its strong exothermic behavior, high vacuum with additionally autoclave processing and high curing temperature (higher than 200 °C) requirements. Recent open literature provides the measured dielectric characteristics of quartz/cyanate ester composite laminate materials at 300 MHz ($\epsilon_{r, comp} = 3.42$ and $\tan\delta_{comp} = 5.8 \times 10^{-3}$ [34]). The quartz/urethane acrylate composite laminates studied here exhibit higher dielectric performance at the same operating frequency: $\epsilon_{r, comp} = 3.1$ and $\tan\delta_{comp} \approx 2.8 \times 10^{-3}$. At higher operating frequency, a study presents the quartz/cyanate ester composite laminates as the combination providing the lowest loss achievable from commercial off-the-shelf aerospace materials with $\tan\delta_{comp} = 3 \times 10^{-3}$ at 10 GHz [13]. For comparison, our quartz/urethane acrylate composite laminates exhibit a loss value $\tan\delta_{comp} = 6 \times 10^{-3}$ at 18 GHz, demonstrating the relevance of such composite materials over a wide operating frequency band, from 100 MHz up to 26 GHz.

7. Conclusions

Dielectric characteristics, namely relative permittivity $\epsilon_{r, comp}$ and loss tangent $\tan\delta_{comp}$, of low loss composite laminate materials were theoretically and experimentally studied at microwaves. The two-dimensional Maxwell-Garnett mixing rule developed for such a material provides fair ($\epsilon_{r, comp}$; $\tan\delta_{comp}$) theoretical values, which fit strongly with the measured ones in the 100 MHz to 1 GHz frequency band (in the uncertainty range of measurement). Mechanical characteristics of the composite laminates were also measured through tensile tests.

This study highlighted the quartz fabric/urethane acrylate type resin composite laminate materials which exhibit ($\epsilon_{r, comp} = 3.1$; $\tan\delta_{comp} = 3.1 \times 10^{-3}$) and ($\epsilon_{r, comp} = 3.2$; $\tan\delta_{comp} = 6 \times 10^{-3}$) mea-

sured values at 1 GHz and 18 GHz, respectively. Such composite laminate materials are therefore relevant for low loss load-bearing antenna composite structures for microwave applications, in direct competition with the quartz fabric/cyanate ester type resin composite laminates. Indeed, this well-known composite material remains more expensive and difficult to implement. Urethane acrylate could therefore be considered as the promising thermosetting resin for substrates and/or radomes of antennas embedded into load-bearing composite panels.

Declaration of Competing Interest

The authors declare that they have no known competing financial interests or personal relationships that could have appeared to influence the work reported in this paper.

Funding

This work was supported in part by the DGA, in part by the Régions Pays-de-la-Loire and Bretagne, in part by the Département des Côtes d'Armor, the Saint-Brieuc Armor Agglomération, and the Lannion-Trégor Communauté, through the FUI'23 STARCOM project. This work was also supported in part by the European Union through the European Regional Development Fund, in part by the Ministry of Higher Education and Research, in part by the Région Bretagne, and in part by the Département des Côtes d'Armor and Saint-Brieuc Armor Agglomération, through the CPER Projects 2015-2020 MATECOM and SOPHIE/STIC & Ondes.

Acknowledgements

The authors warmly acknowledge F. Boutet from IETR and ID Composite team for their technical supports.

References

- [1] A.D.B.L. Ferreira, P.R.O. Nóvoa, A.T. Marques, Multifunctional material systems: a state-of-the-art review, *Compos. Struct.* 151 (2016) 3–35 <https://doi.org/10.1016/j.compstruct.2016.01.028>.
- [2] K.K. Sairajan, G.S. Aglietti, K.M. Mani, A review of multifunctional structure technology for aerospace applications, *Acta Astronaut.* 120 (2016) 30–42 <https://doi.org/10.1016/j.actaastro.2015.11.024>.
- [3] T. Pereira, Z. Guo, S. Nieh, J. Arias, H.T. Hahn, Embedding thin-film lithium energy cells in structural composites, *Compos. Sci. Technol.* 68 (2008) 1935–1941 <https://doi.org/10.1016/j.compscitech.2008.02.019>.

- [4] T. Seong Jang, D. Soo Oh, J. Kyu Kim, K. In Kang, W. Ho Cha, S. Woo Rhee, Development of multi-functional composite structures with embedded electronics for space application, *Acta Astronaut.* 68 (2011) 240–252 <https://doi.org/10.1016/j.actaastro.2010.08.009>.
- [5] C.S. You, W. Hwang, Design of load-bearing antenna structures by embedding technology of microstrip antenna in composite sandwich structure, *Compos. Struct.* 71 (2005) 378–382 <https://doi.org/10.1016/j.compstruct.2005.09.021>.
- [6] J. Kim, J.-Y. Jang, G.-H. Ryu, J.-H. Choi, M.-S. Kim, Structural design and development of multiband aero-vehicle smart skin antenna, *J. Intell. Mater. Syst. Struct.* 25 (2014) 631–639 <https://doi.org/10.1177/1045389X13493358>.
- [7] L. Manac'h, X. Castel, M. Himdi, Performance of a lozenge monopole antenna made of pure composite laminate, *Prog. Electromagn. Res. Lett.* 35 (2012) 115–123 <https://doi.org/10.2528/PIERL12083003>.
- [8] C.S. You, R.M. Lee, W. Hwang, H.C. Park, W.S. Park, Microstrip antenna for SAR application with microwave composite laminates and honeycomb cores, in: *13th Int. Conf. Compos. Mater.*, 2001, pp. 1–10.
- [9] L. Yao, M. Jiang, D. Zhou, F. Xu, D. Zhao, W. Zhang, N. Zhou, Q. Jiang, Y. Qiu, Fabrication and characterization of microstrip array antennas integrated in the three dimensional orthogonal woven composite, *Compos. Part B Eng.* 42 (2011) 885–890 <https://doi.org/10.1016/j.compositesb.2011.01.006>.
- [10] F. Xu, L. Yao, D. Zhao, M. Jiang, Y. Qiu, Effect of a surface resin layer covering the radiating patch on performance of a three dimensional integrated microstrip antenna, *J. Compos. Mater.* 45 (2011) 1627–1635 <https://doi.org/10.1177/0021998310387670>.
- [11] J. Zhou, J. Huang, L. Song, D. Zhang, Y. Ma, Electromechanical co-design and experiment of structurally integrated antenna, *Smart Mater. Struct.* 24 (2015) 037004 <https://doi.org/10.1088/0964-1726/24/3/037004>.
- [12] K. Naito, Y. Kagawa, K. Kurihara, Dielectric properties and noncontact damage detection of plain-woven fabric glass fiber reinforced epoxy matrix composites using millimeter wavelength microwave, *Compos. Struct.* 94 (2012) 695–701 <https://doi.org/10.1016/j.compstruct.2011.09.002>.
- [13] T.C. Baum, K. Ghorbani, A. Galehdar, K.J. Nicholson, R.W. Ziolkowski, Multi-functional composite metamaterial-inspired EAD antenna for structural applications, in: *2016 Int. Work. Antenna Technol. IWAT 2016*, 2016, pp. 144–147. <https://doi.org/10.1109/IWAT.2016.7434826>.
- [14] Keysight, Data sheet - Agilent E4991A RF Impedance / Material analyzer. <https://www.keysight.com/en/pd-1000003705:epsg:pro-pn-E4991A/rf-impedance-material-analyzer?&cc=FR&lc=fr>, 2011 (accessed 8 Jun 2020).
- [15] AFNOR, European Standard NF EN ISO 527-4, 1997.
- [16] H. Schreier, J.-J. Orteu, M.A. Sutton, *Image Correlation for Shape, Motion and Deformation Measurements*, Springer US, Boston, MA, 2009 <https://doi.org/10.1007/978-0-387-78747-3>.
- [17] K.K. Chawla, *Composite Materials*, Springer, New York, New York, NY, 2012 <https://doi.org/10.1007/978-0-387-74365-3>.
- [18] JPS, Catalogue 2017. <https://3td3dv4djc4f218gpz1bk9c4-wpengine.netdna-ssl.com/wp-content/uploads/2017/10/2017-Data-Book-Small-1-1.pdf>, 2017 (accessed 8 Jun 2020)
- [19] Composite materials Handbook - Polymer matrix composites / Materials usage, design, and analysis, vol. 3, US Dept of Defense, 2002. <https://www.library.ucdavis.edu/wp-content/uploads/2017/03/HDBK17-3F.pdf> (accessed 8 Jun 2020).
- [20] J.C. Maxwell Garnett, Colours in metal glasses and in metallic films, *Philos. Trans. R. Soc. A Math. Phys. Eng. Sci.* 203 (1904) 385–420 <https://doi.org/10.1098/rsta.1904.0024>.
- [21] K. Wu, J. Li, K. von Salzen, F. Zhang, Explicit solutions to the mixing rules with three-component inclusions, *J. Quant. Spectrosc. Radiat. Transf.* 207 (2018) 78–82 <https://doi.org/10.1016/j.jqsrt.2017.12.020>.
- [22] M.A. Benali, H. Tabet Derraz, I. Ameri, A. Bourguig, A. Neffah, R. Miloua, I.E. Yahiaoui, M. Ameri, Y. Al-Douri, Synthesis and analysis of SnO₂/ZnO nanocomposites: structural studies and optical investigations with Maxwell-Garnett model, *Mater. Chem. Phys.* 240 (2019) 1–7 <https://doi.org/10.1016/j.matchemphys.2019.122254>.
- [23] Y. Yao, J. Luo, X. Duan, T. Liu, Y. Zhang, B. Liu, M. Yu, On the piezoresistive behavior of carbon fibers – cantilever-based testing method and Maxwell-Garnett effective medium theory modeling, *Carbon* 141 (2019) 283–290 <https://doi.org/10.1016/j.carbon.2018.09.043>.
- [24] V.A. Markel, Introduction to the Maxwell Garnett approximation: tutorial, *J. Opt. Soc. Am. A* 33 (2016) 1244 <https://doi.org/10.1364/JOSAA.33.001244>.
- [25] D.A.G. Bruggeman, Berechnung verschiedener physikalischer Konstanten von heterogenen Substanzen, *Ann. Phys.* 416 (1935) 636–664 <https://doi.org/10.1002/andp.19354160705>.
- [26] Z. Hashin, S. Shtrikman, A variational approach to the theory of the effective magnetic permeability of multiphase materials, *J. Appl. Phys.* 33 (1962) 3125–3131 <https://doi.org/10.1063/1.1728579>.
- [27] O. Wiener, *Zur theorie der refraktionskonstanten*, 1910.
- [28] K. Bal, V. Kothari, Permittivity of woven fabrics: a comparison of dielectric formulas for air-fiber mixture, *IEEE Trans. Dielectr. Electr. Insul.* 17 (2010) 881–889 <https://doi.org/10.1109/TDEI.2010.5492262>.
- [29] W.S. Chin, D.G. Lee, Binary mixture rule for predicting the dielectric properties of unidirectional E-glass/epoxy composite, *Compos. Struct.* 74 (2006) 153–162 <https://doi.org/10.1016/j.compstruct.2005.04.008>.
- [30] A.H. Sihvola, Mixing rules with complex dielectric coefficients, *Subsurf. Sens. Technol. Appl.* 1 (2000) 393–415 <https://doi.org/10.1023/A:1026511515005>.
- [31] V.I. Kostikov, *Fibre Science and Technology*, Springer, Netherlands, 2012 <https://doi.org/10.1007/978-94-011-0565-1>.
- [32] K.K. Kärkkäinen, A.H. Sihvola, K.I. Nikoskinen, Effective permittivity of mixtures: numerical validation by the FDTD method, *IEEE Trans. Geosci. Remote Sens.* 38 (2000) 1303–1308 <https://doi.org/10.1109/36.843023>.
- [33] M.T. Sebastian, Measurement of microwave dielectric properties and factors affecting them, in: Elsevier (Ed.), *Dielectr. Mater. Wirel. Commun.*, Elsevier, Amsterdam, 2008, pp. 11–47. <https://doi.org/10.1016/B978-0-08-045330-9.00002-9>.
- [34] T.C. Baum, R.W. Ziolkowski, K. Ghorbani, K.J. Nicholson, Investigations of a load-bearing composite electrically small egyptian axe dipole antenna, *IEEE Trans. Antennas Propag.* 65 (2017) 3827–3837 <https://doi.org/10.1109/TAP.2017.2708122>.